JACS
JOURNAL OF THE AMERICAN CHEMICAL SOCIETY
Article
pubs.acs.org/JACS

Why Bistetracenes Are Much Less Reactive Than Pentacenes in Diels–Alder Reactions with Fullerenes

Yang Cao,[†] Yong Liang,[†] Lei Zhang,[‡] Sílvia Osuna,[†] Andra-Lisa M. Hoyt,[‡] Alejandro L. Briseno,*[,‡] and K. N. Houk*[,†]

[†]Department of Chemistry and Biochemistry, University of California, Los Angeles, California 90095, United States
[‡]Department of Polymer Science & Engineering, Conte Polymer Research Center, University of Massachusetts, Amherst, Massachusetts 01003, United States

Supporting Information

ABSTRACT: The Diels–Alder (DA) reactions of pentacene (PT), 6,13-bis(2-trimethylsilylethynyl)pentacene (TMS-PT), bistetracene (BT), and 8,17-bis(2-trimethylsilylethynyl)bistetracene (TMS-BT) with the [6,6] double bond of [60]fullerene have been investigated by density functional theory calculations. Reaction barriers and free energies have been obtained to assess the effects of frameworks and substituent groups on the DA reactivity and product stability. Calculations indicate that TMS-BT is about 5 orders of magnitude less reactive than TMS-PT in the reactions with [60]fullerene. This accounts for the observed much higher stability of TIPS-BT than TIPS-PT when mixed with PCBM. Surprisingly, calculations predict that the bulky silylethynyl substituents of TMS-PT and TMS-BT have only a small influence on reaction barriers. However, the silylethynyl substituents significantly destabilize the corresponding products due to steric repulsions in the adducts. This is confirmed by experimental results here. Architectures of the polycyclic aromatic hydrocarbons (PAHs) play a crucial role in determining both the DA barrier and the adduct stability. The reactivities of different sites in various PAHs are related to the loss of aromaticity, which can be predicted using the simple Hückel molecular orbital localization energy calculations.

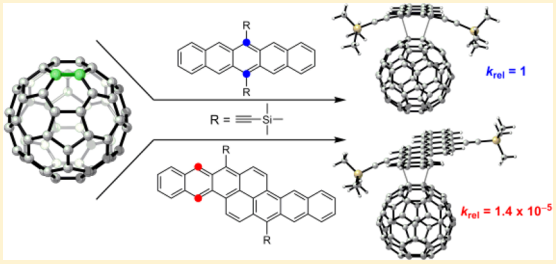

INTRODUCTION

Polycyclic aromatic hydrocarbons (PAHs) composed of linearly fused benzene rings have been widely explored as organic semiconductor materials for their unique electronic properties.[1] Pentacene (PT) is among the most well-studied molecules and has emerged as a promising donor material for organic photovoltaic (OPV) devices due to its significantly large exciton diffusion length[2] and high hole mobility.[3] PT is also studied as the model system for calculating exciton-dissociation and charge-recombination processes.[4] More recently, the quantum efficiency of pentacene/fullerene-based OPVs was significantly improved by the singlet exciton fission effect.[5] Despite great progress, there is a fundamental problem regarding the chemical stability of pentacene systems that requires further investigation. Pentacene is unstable in air or visible light, suffering from oxidation and rapid conversion to transannular peroxides.[6] It has extremely poor solubility in organic solvents,[7] which makes it useless for large-area, solution-based applications. Pentacene has been found to be highly reactive as a diene in Diels–Alder (DA) reactions with [60]fullerene. Miller and co-workers reported that the DA reaction of fullerene with pentacene in solution yields the C_{2v}-symmetric monoadduct across the central 6,13-carbons of pentacene.[8] They also found that, when the reactive 6,13-positions on pentacene are substituted, C_{60} reacts with pentacene at the 5,14- and 7,12-positions to generate bis- and monofullerene adducts.[9] One example is 6,13-bis(2-trimethylsilylethynyl)pentacene (TMS-PT, Figure 1).[9b] The reaction of TMS-PT with excess fullerene in CS_2 leads to a monoadduct across the 5,14-carbons after 24 h. Bisfullerene–pentacene adducts also form after longer reaction times (2–3 days). In fact, the DA reactions between pentacene and its

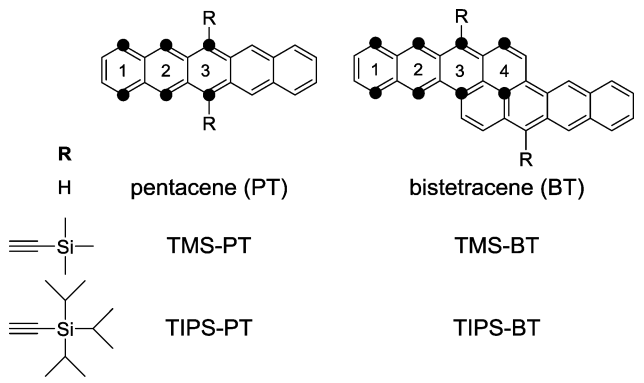

Figure 1. Structures of pentacene, bistetracene, and their derivatives with their reaction sites as dienes in Diels–Alder reactions.

Received: May 25, 2014
Published: July 9, 2014

dx.doi.org/10.1021/ja505240e | J. Am. Chem. Soc. 2014, 136, 10743–10751

derivatives with fullerene are so efficient that they have been applied as methods to synthesize functional fullerene materials.[9c,d]

In the search for alternative air-stable, solution-processable, highly crystalline organic materials for electronic device applications, substituents such as silylethynyl, aryl, and alkyl groups have been introduced on pentacene backbones.[1,10] In general, the substituted pentacenes are more stable and more soluble than the parent compound, but many have the disadvantages of minimal π-stacking and poorer device performance.[11] Other PAHs have been designed to achieve desirable electronic properties and chemical stability.[12] Recently, the Briseno group synthesized and characterized bistetracene (BT) and its derivative, triisopropylsilylethynyl-substituted bistetracene (TIPS-BT, Figure 1).[13] TIPS-BT is reported to have a half-life of 4 days under UV/vis irradiation in chloroform, which is about 200 times longer than the half-life of pentacene. Further investigation showed that the BT derivative has promising properties, such as small band gap and high carrier mobilities up to 6 $cm^2/(V{\cdot}s)$.[13]

To compare the stability between TIPS-PT and TIPS-BT (Figure 1) in the fullerene system, the reactions of these compounds with [6,6]-phenyl-C_{61}-butyric acid methyl ester (PCBM) were carried out in $CDCl_3$ under ambient conditions and monitored by ^1H NMR (for details, see the Supporting Information). As shown in Figure 2a, the DA reaction between TIPS-PT and PCBM is very fast, and several new signals can be observed within a few minutes. This is consistent with previous reports regarding the propensity of pentacene derivatives to undergo DA reactions with fullerene derivatives.[8,9] By contrast, the NMR spectra of mixed TIPS-BT and PCBM show almost no observable change in the first 36 h (Figure 2b). There are a few signal changes after longer reaction time (>48 h). This indicates that the DA reaction of TIPS-BT with PCBM is much slower than that of TIPS-PT.

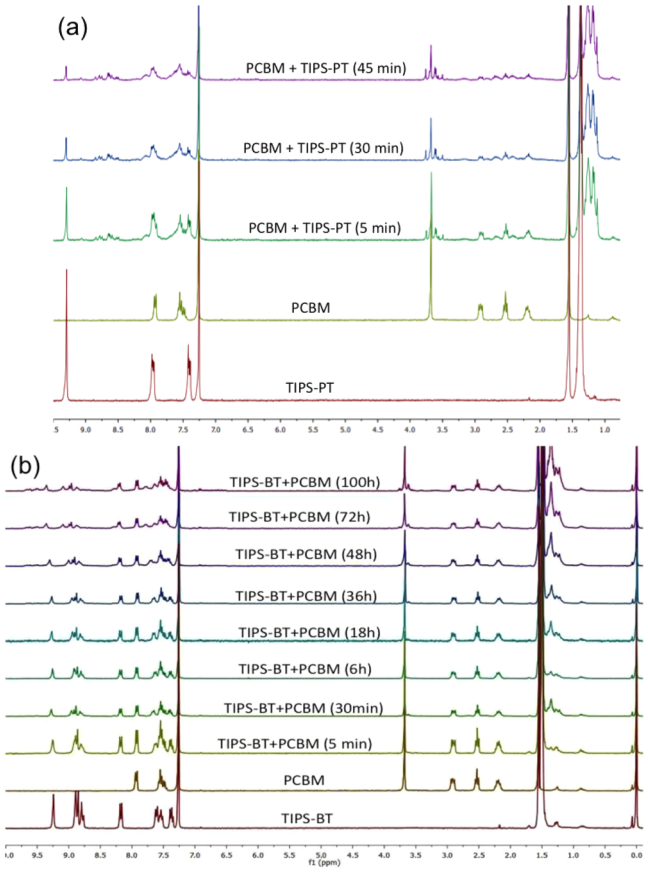

Figure 2. ^1H NMR spectra at various time intervals of TIPS-PT (a) and TIPS-BT (b) mixed with PCBM in $CDCl_3$ at room temperature.

These promising results stimulated the Briseno group to investigate other conjugated PAH derivatives that have appropriate properties with sufficient chemical inertness to be used in OPV devices.[12] To enable rational design of new molecules, there is the need to improve the understanding of the influence of both substituent groups and frameworks on stabilities of potential organic electronic materials.

These factors have been analyzed here by density functional theory (DFT) and Hückel molecular orbital (HMO) calculations. We show here that the BT system is significantly less reactive than pentacene, since it is more difficult to interrupt the aromatic conjugation of the more highly condensed benzene rings of BT. The rate of the DA reaction between the fullerene and TMS-BT is predicted to be 70 000 times slower than that of TMS-PT molecule at 25 °C. The introduction of bulky silylethynyl groups on site 3 (Figure 1) in PT and BT molecules is surprisingly found to only slightly influence the DA barriers on site 3, but to destabilize the corresponding products substantially. The localization energies obtained from HMO methods are found to correlate with the activation free energies and reaction free energies from DFT calculations on the DA reactions of fullerene with PT and BT. As has been described for other DA reactions of polyacenes,[14] the HMO localization energies of different sites in various PAHs can be used to estimate the reactivities of PAHs.

COMPUTATIONAL METHODS

The DFT calculations were all performed with the Gaussian 09 programs.[15] Recently, DFT calculations of cycloaddition reactions on carbon nanotubes were reported,[16] where optimizations were performed at the B3LYP/3-21G* level.[17,18] We started our geometry optimizations with the same method and basis set, followed by single point calculations at the B3LYP/6-31G(d) level. However, the B3LYP results significantly underestimate observed reactivities. For pentacene, the DA reaction between site 3 (Figure 1) and the [6,6] bond of [60]fullerene was reported to occur rapidly.[8] However, the B3LYP calculations gave an activation free energy of over 32 kcal/mol and an endergonic product with a reaction energy of 5.8 kcal/mol. This experimental and theoretical difference is consistent with previous discoveries that B3LYP failed to give reliable energetics for medium- to long-range electron correlations and dispersion effects.[19,20] The M06-2X method[21] was demonstrated to yield more accurate energetics for such systems and cycloaddition reactions.[22] The performance of M06-2X has been verified on graphene chemistry.[23] Consequently, we have performed optimizations at the M06-2X/3-21G* level. The vibrational frequencies were computed at the same level to ensure each optimized structure is an energy minimum or a transition state and to evaluate zero-point vibrational energies (ZPVE) and thermal corrections at 298 K. Single-point energy calculations in $CHCl_3$ using the CPCM model[24] were carried out subsequently on the optimized structures at the M06-2X with a larger basis set 6-31G(d). We tested optimizations at the M06-2X/6-31G(d) level for the [60]fullerene–pentacene system. The differences in both activation free energies and reaction free energies are less than 1.0 kcal/mol. In addition, we tested single point energy calculations at the B3LYP-D3/6-31G(d) or BP86-D3/6-31G(d) level for all the investigated systems (for details, see Table S1 in the Supporting Information).

We calculated the DA reactions of [60]fullerene with polycyclic aromatics, PT, TMS-PT, BT, and TMS-BT. Their structures and DA reaction sites are shown above in Figure 1, and the structures of

dx.doi.org/10.1021/ja505240e | J. Am. Chem. Soc. 2014, 136, 10743–10751

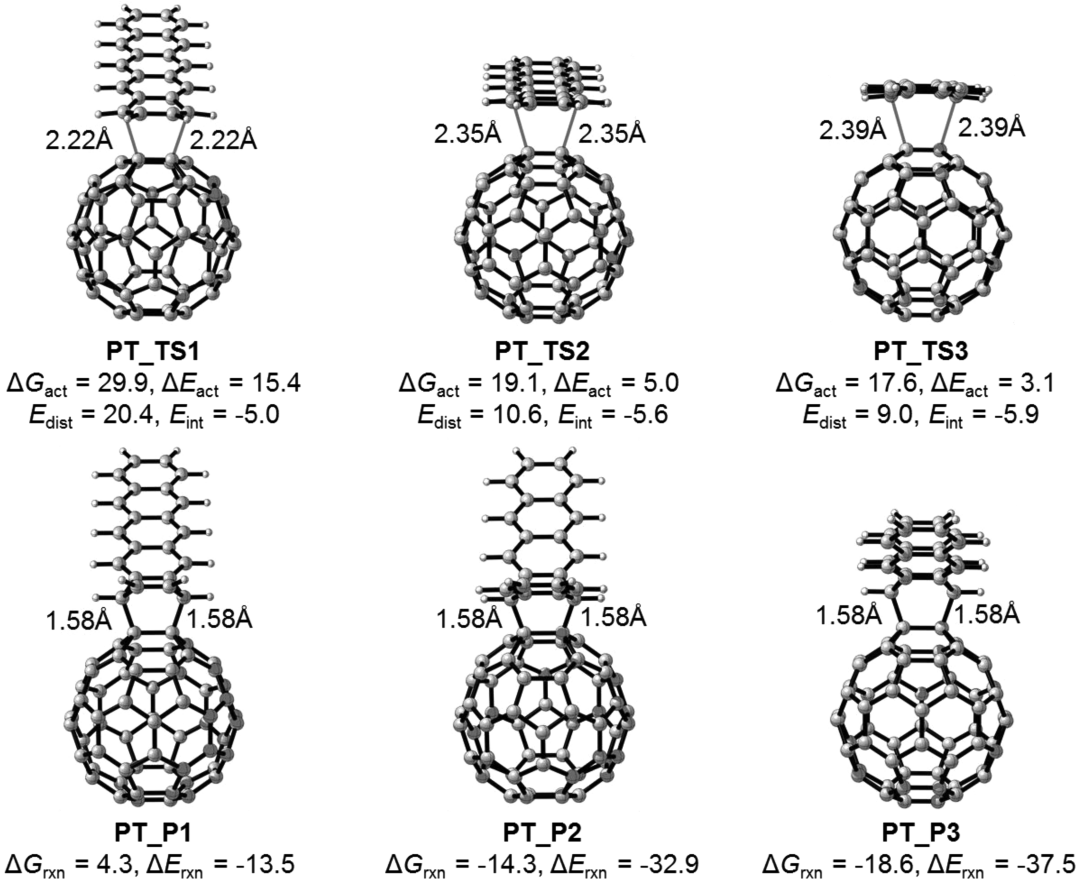

Figure 3. Free energies and distortion/interaction analysis for the C_{60}-PT reactions (energies in kcal/mol).

transition states and products are given below in Figures 3, 4, 6, and 7. Substituent effects were assessed by comparing PT/BT and TMS-PT/TMS-BT systems. The effects of additional fused aromatic rings were evaluated through the comparison of PT and BT systems.

Solà and co-workers reported the enthalpies of DA reactions involving C_{60}.[19a] The optimized reactant complexes were local minima and were stabilized by 4−12 kcal/mol in enthalpy with respect to separated reactants. We also considered the complexes between C_{60} and four PAHs and observed the same stabilization effect of 8−12 kcal/mol in enthalpy, due primarily to dispersion interactions.[25] Here we report energy profiles in terms of Gibbs free energy. In the free energy ($\Delta G = \Delta H - T\Delta S$), the entropy term ($-T\Delta S$ is positive) causes the free energies of these four complexes to actually be higher than those of separated reactants. As a result, the energies discussed in the text are all given relative to separated fullerene and PAHs.

We also analyzed the activation barriers using the distortion/interaction model.[26,27] This model relates the activation energy (E_{act}) to the distortion energy (E_{dist}) required for the geometrical deformation of the reactants to achieve their transition-state conformations and the interaction energy (E_{int}) arising from the interactions between two distorted reactants in the transition state.[28] Fragment distortion and interaction energies were computed at the M06-2X/6-31G(d) level in the gas phase. In all cases, the distortion energies of PAHs are predominant, around 75% of the total distortion energies.

RESULTS AND DISCUSSION

It is well established both experimentally and computationally that the DA reaction of fullerene occurs on a [6,6] double bond (located between two fused 6-membered rings).[28g,29] Our calculations indicate that the reaction barriers on the [5,6] bond (where 5- and 6-membered rings are fused) are about 14 kcal/mol higher than those on the [6,6] bond (for details, see Figure S1 in the Supporting Information). Therefore, we only discuss the DA reactions on a [6,6] bond of fullerene here.

Figure 3 shows the DA transition states and products involving pentacene (PT) and the [6,6] bond of fullerene. Site 3 is the most reactive site of PT as the diene, where the DA barrier is only 17.6 kcal/mol. The free energy barrier on site 2 is slightly higher (19.1 kcal/mol). Site 1 has the highest reaction barrier of 29.9 kcal/mol. According to the distortion/interaction analysis, the interaction energies (E_{int}) for three transition states are very close, between −5.0 and −5.9 kcal/mol. The distortion energies (E_{dist}) are related to the position of transition states, measured as the partially formed C−C bond length. The distortion energies control activation barriers. Smaller distortion energies lead to lower activation energies. It is easiest to interrupt the aromatic system of pentacene on site 3. This corresponds to the earliest transition state (**PT_TS3**) with longest forming C−C bonds (2.39 Å) and thus the smallest transition-state distortion energy (E_{dist}) of 9.0 kcal/mol. Site 1 has the highest reaction barrier, and formation of the DA adduct is endergonic. Its transition state has the shortest forming C−C bonds (2.22 Å) and the largest distortion energy (20.4 kcal/mol). The C−C bond lengths on site 2 are intermediate, with a distortion energy of 10.6 kcal/mol. The adduct on site 3 (**PT_P3**) is the most stable one with a reaction free energy of −18.6 kcal/mol. The adduct on site 2 (**PT_P2**) is less exergonic, with a free energy of −14.3 kcal/mol. The DA reaction on site 1 is endergonic by 4.3 kcal/mol. Therefore, the DA reaction on site 3 is preferred kinetically, with the earliest transition state, and thermodynamically, with

dx.doi.org/10.1021/ja505240e | J. Am. Chem. Soc. 2014, 136, 10743−10751

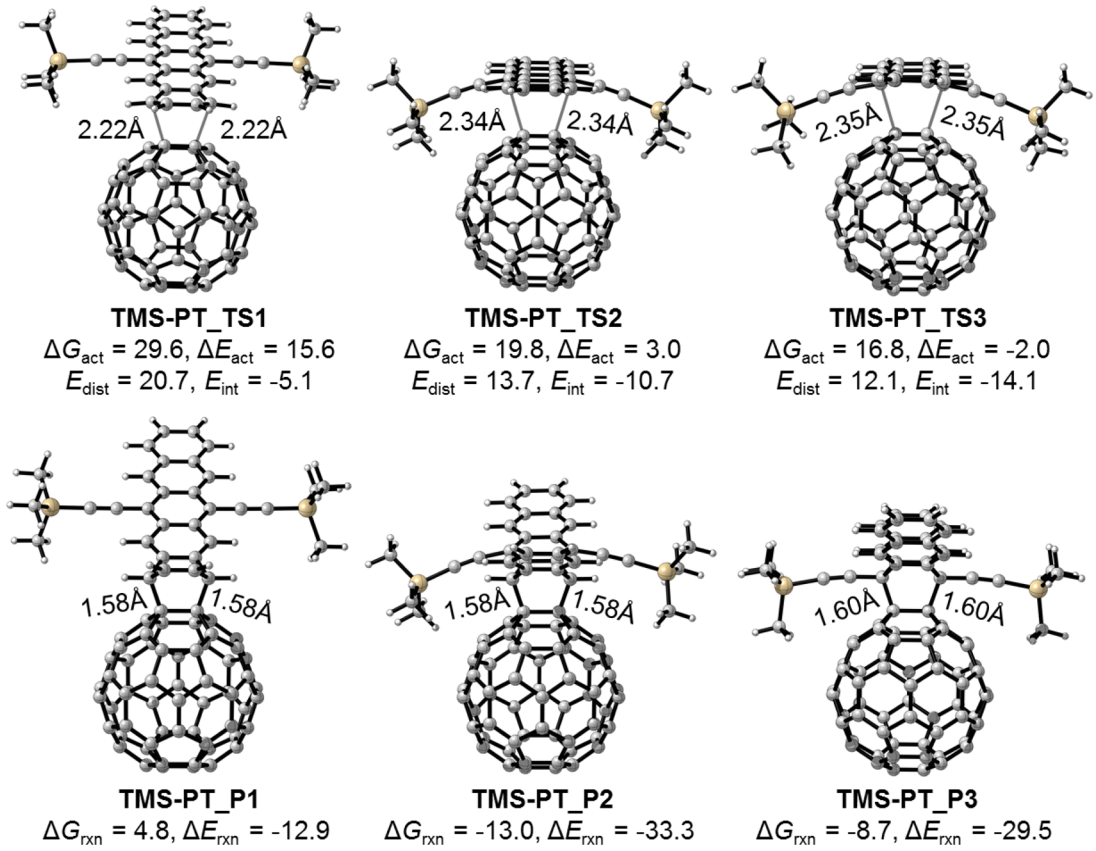

Figure 4. Free energies and distortion/interaction analysis for the C_{60}-TMS-PT reactions (energies in kcal/mol).

the most exergonic product.[30] This result is in agreement with the experiment that pentacene reacts rapidly with C_{60} through the DA reaction across the central 6,13-carbons.[8]

Figure 4 shows the DA transition states and products from reactions of TMS-PT and [60]fullerene. The introduction of the trimethylsilylethynyl substituent groups does not have a significant effect on the DA reactivity. The barriers for reactions on sites 1−3 of TMS-PT are very close to those of PT. Site 3 in TMS-PT is the most reactive one among the three sites with an activation free energy of 16.8 kcal/mol. This barrier is even slightly lower than that for pentacene via transition state **PT_TS3** (17.6 kcal/mol, Figure 3). This indicates that the reaction of TMS-PT with C_{60} will be quite fast at room temperature. The reaction on site 2 via **TMS-PT_TS2** requires an activation free energy of 19.8 kcal/mol, which is 3.0 kcal/mol higher than that on site 3 via **TMS-PT_TS3**. The reaction on site 1 has the highest barrier of 29.6 kcal/mol. The distortion/interaction analysis shows that both interaction energies (E_{int}) and distortion energies (E_{dist}) vary with the length of the forming C−C bonds. The longer the C−C bonds, the lower the distortion energies. Similar to pentacene, site 3 has the earliest transition state with the longest C−C bonds (2.35 Å). The distortion energy of transition state **TMS-PT_TS3** is 12.1 kcal/mol. The transition state on site 2 is intermediate with slightly shorter C−C bonds of 2.34 Å. Site 1 has the latest transition state with the shortest C−C bonds (2.22 Å), which leads to more severe distortion energy of 20.7 kcal/mol. The interaction energies become more favorable as bond length elongates. It ranges from −5.1 kcal/mol on site 1 to −10.7 kcal/mol on site 2 to −14.1 kcal/mol on site 3. The stabilizing dispersion interactions between TMS-PT and fullerene mainly contribute to the interaction energies. There is a better alignment in **TMS-PT_TS3**, and thus it has an enhanced stabilizing dispersion between TMS-PT and fullerene.

Similar to PT, the DA reaction of TMS-PT on site 1 is endergonic by 4.8 kcal/mol. However, the stability of the products on sites 2 and 3 is reversed by the bulky side groups (Figures 3 and 4). The reaction free energy of adduct **TMS-PT_P2** is −13.0 kcal/mol, 4.3 kcal/mol more favorable than that of adduct **TMS-PT_P3** on site 3 (−8.7 kcal/mol, Figure 4). As shown in Figures 3 and 4, five out of six DA adducts have formed C−C bonds of 1.58 Å. To avoid the large steric repulsions between the bulky silylethynyl groups of TMS-PT and fullerene, the adduct on site 3 has to stretch the formed C−C bonds to 1.60 Å. This significantly destabilizes the product **TMS-PT_P3**.

The DA reaction between TMS-PT and C_{60} was reported by Miller's group.[9b] The monoadduct across the site 2 (**TMS-PT_P2**) was obtained in a yield of 75% after refluxing in CS_2 for 24 h, while the adduct across the site 3 (**TMS-PT_P3**) was not isolated. This is consistent with the computational result that the DA reaction on site 2 is thermodynamically much more favorable. However, calculations indicate that the formation of adduct on site 3 is preferred kinetically. To test this prediction, we conducted the reaction of TIPS-PT with C_{60} in a $CDCl_3$/CS_2 mixed solution at room temperature and monitored it by ^{1}H NMR (Figure 5; for details, see the Supporting Information). As expected, it was found that about half of TIPS-PT was converted into the fullerene monoadduct on site 3 (**TIPS-PT_P3**) in 5 min with almost no signals of the adduct on site 2 (**TIPS-PT_P2**, Figure 5). This shows that the DA

dx.doi.org/10.1021/ja505240e | J. Am. Chem. Soc. 2014, 136, 10743−10751

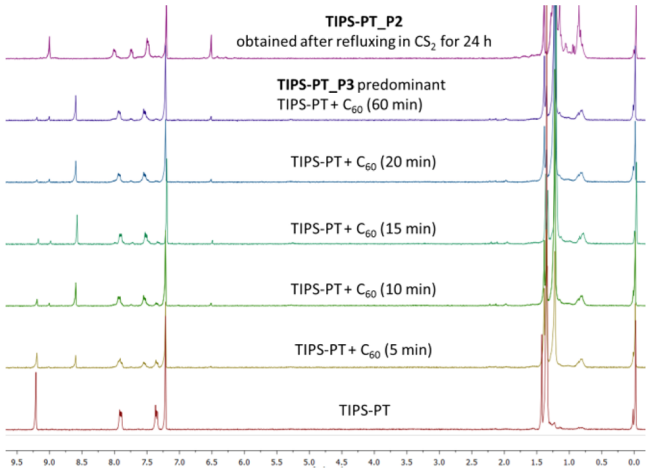

Figure 5. ^{1}H NMR spectra at various time intervals of TIPS-PT mixed with C_{60} in $CDCl_3/CS_2$ at room temperature.

reaction of fullerene on site 3 of silylethynyl substituted pentacene is still much faster than that on site 2, although the adduct on site 3 is less stable.

As shown in Figure 6, for the BT molecule, the DA barriers are substantially higher than those with the PT molecule. The two-row fused aromatic ring framework deactivates the whole system. Site 2 is the most reactive one among four possible reaction sites (Figure 1), requiring an activation free energy of 22.1 kcal/mol. The reaction on site 3 has a similar barrier of 23.1 kcal/mol. The reaction barriers on sites 1 and 4 are much higher, 31.4 and 37.1 kcal/mol, respectively. Site 2 has the earliest transition state with the lowest distortion energy of 13.4 kcal/mol. For products, only the adduct on site 2 is formed exergonically, with a free energy of −8.3 kcal/mol. The formation of the product on site 3 is endergonic by 2.2 kcal/mol. This implies that retro-DA reaction on site 3 is faster than the forward DA reaction. Even with a surmountable transition barrier, **BT_P3** is highly unstable and easily decomposes. The reaction free energies on sites 1 and 4 are even more endergonic.

Figure 7 shows the DA transition states and adducts involving four reaction sites of TMS-BT and fullerene. Very similar to the BT molecule, the reaction on site 2 has the lowest free energy barrier, 23.4 kcal/mol. The final adduct can only be formed on site 2 with a reaction free energy of −7.3 kcal/mol. The trimethylsilylethynyl groups make the DA adduct on site 3 (**TMS-BT_P3**) much more unfavorable, with a free energy of 8.4 kcal/mol above the reactants. Comparing the free energy of **TMS-BT_P3** and **BT_P3**, an additional side group destabilizes the product by 6.2 kcal/mol (8.4 versus 2.2 kcal/mol, Figures 7 and 6). Therefore, the DA reaction on site 2 of TMS-BT is preferred both kinetically and thermodynamically.

In summary, for pentacene, the reaction across central 6,13-carbons is preferred both kinetically and thermodynamically. Adding bulky substituent groups on these two carbons does little to the transition state energy but decreases the product stability by about 10 kcal/mol. This is confirmed by experimental results here (Figure 5). Similarly, for BT, one side group on site 3 reduces the stability of the corresponding product by about 6 kcal/mol. Therefore, the introduction of

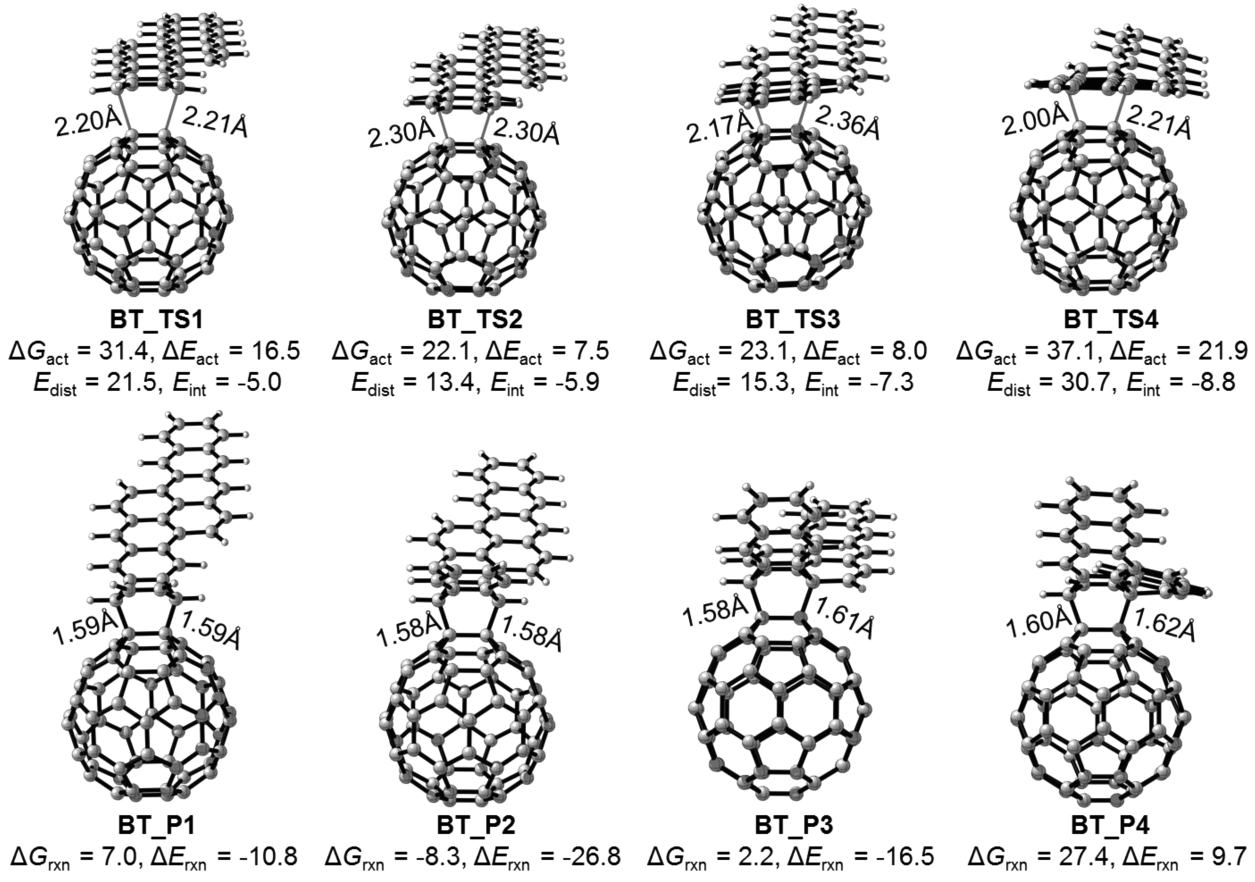

Figure 6. Free energies and distortion/interaction analysis for the C_{60}-BT reactions (energies in kcal/mol).

dx.doi.org/10.1021/ja505240e | J. Am. Chem. Soc. 2014, 136, 10743−10751

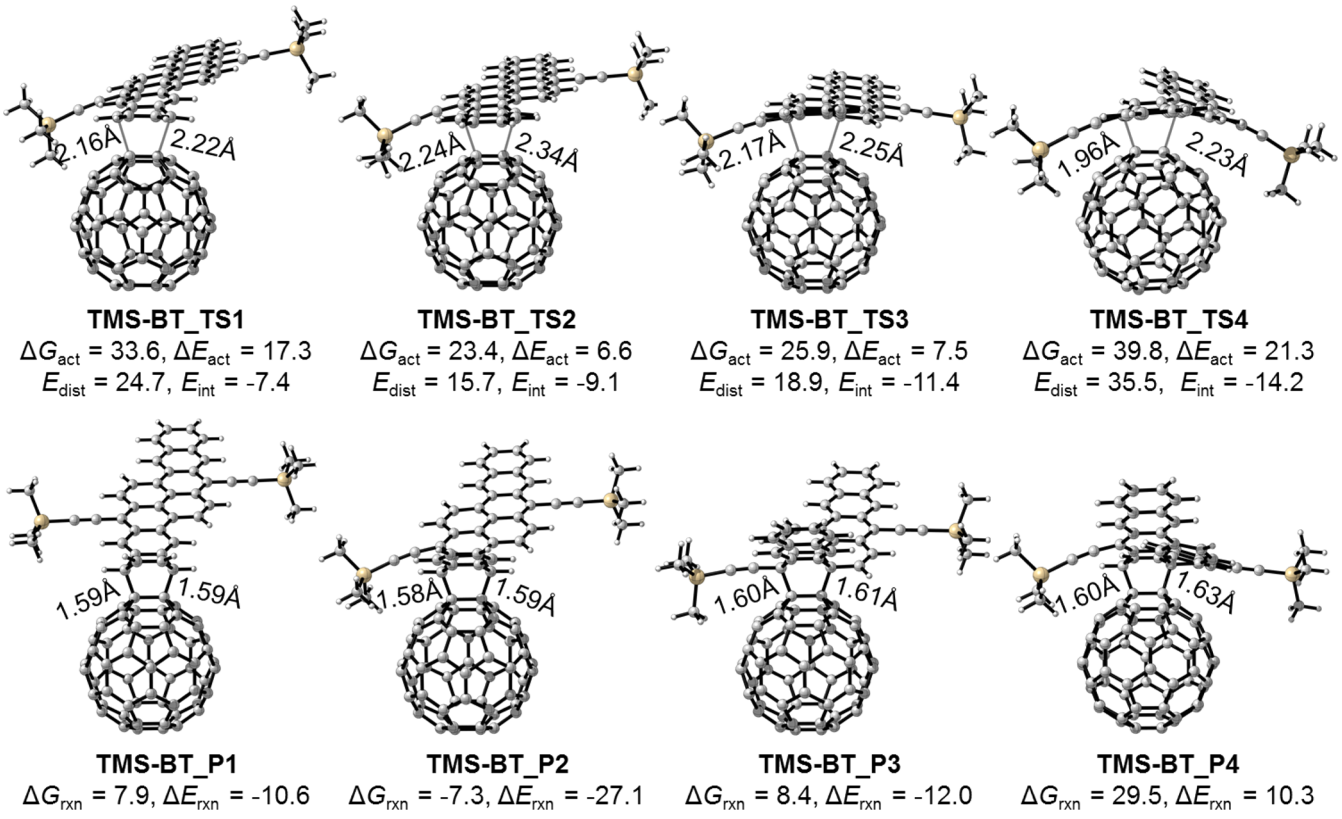

Figure 7. Free energies and distortion/interaction analysis for the C_{60}-TMS-BT reactions (energies in kcal/mol).

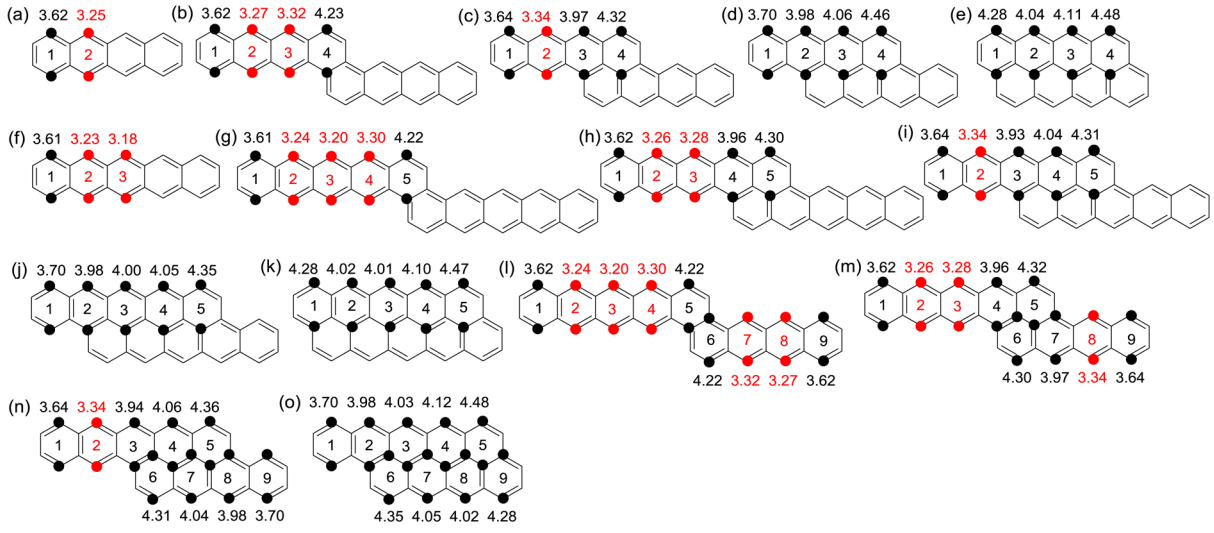

Figure 8. HMO 1,4-localization energies for different PAHs (in units of $-\beta$).

each bulky group decreases the stability of adduct on the substituted carbon site by approximately 5 kcal/mol. The lowest energy DA transition states for TMS-PT and TMS-BT molecules are **TMS-PT_TS3** (Figure 4) and **TMS-BT_TS2** (Figure 7), requiring activation free energies of 16.8 and 23.4 kcal/mol, respectively. On the basis of the free energy difference of 6.6 kcal/mol, we predict that TMS-BT is 70 000 times less reactive than TMS-PT in reactions with fullerene. This accounts for the experimental results in Figure 2: the mixed TIPS-BT and PCBM shows almost no signal change until about 2 days, while the reaction between TIPS-PT and PCBM readily occurs within a few minutes.

Relative Reactivities and Stabilities Assessed by HMO Localization Energies. The concept of localization energy was developed by Wheland[31] and Brown[32] in 1940s. By definition, the localization energy (E_L) is the energy difference between the initial π system (E) and that remaining (E_r) after removal of one or more p orbital and electron from the π system: $E_L = E_r - E$. The localization energies were found to correlate with the reactivities in some types of aromatic substitution reactions[32] and DA reactions.[14,33] For different reaction sites in one molecule, the larger E_L is, the more stable the site is and the more difficult the cycloaddition reaction is. The most reactive position has the smallest localization energy.

dx.doi.org/10.1021/ja505240e | J. Am. Chem. Soc. 2014, 136, 10743−10751

The properties and stabilities of large PAHs depend upon the number and the spatial arrangement of benzene rings in their conjugated systems, which are usually associated with their resonance energies. Developed in 1930s, the HMO theory can be applied to calculations of the energies of π electrons in such planar conjugated systems. Schleyer et al. have also explored the relationship between other aromaticity indices and the reactivities of polyacenes in DA reactions.[34]

We recently applied HMO calculations on graphene models and found that the HMO localization energies could predict the reactivities of different graphene sites.[23b] The HMO energies were calculated using the online Hückel program SHMO developed by Arvi Rauk.[35] In the HMO theory, the energy of π electrons is expressed in terms of α and β: $E = n\alpha + \lambda\beta$, where α is the Coulomb integral and β is the resonance integral. Here the localization energies on seven reaction sites within PT and BT molecules (Figure 1) were calculated by HMO theory. Because all seven sites have the same loss in α term, the α term is neglected. The computed 1,4-localization energies (in units of $-\beta$) for PT, BT, and other PAHs are summarized in Figure 8.

Figure 9 shows a plot of DFT activation free energies or reaction free energies versus HMO localization energies for the

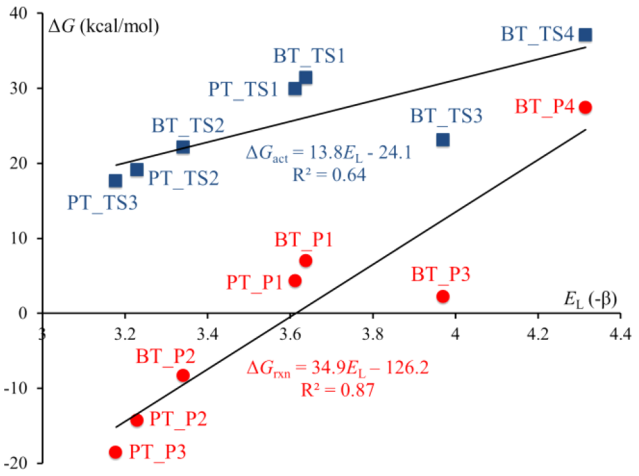

Figure 9. Correlation between HMO localization energies and DFT activation free energies (in blue) or reaction free energies (in red) of DA reactions on seven reaction sites in PT and BT.

DA reactions of seven reaction sites in PT and BT molecules (all seven reactions in Figures 3 and 6). Although some points, such as **BT_TS3** and **BT_P3**, have large deviations from the lines, the overall correlation for reaction free energies is good (R^2 = 0.87). This indicates that the reactivities of different sites in PAHs are mainly determined by the loss of the resonance energies after reactions. Although highly simplified, the HMO localization energy can be used as a tool to estimate the reactivities of various PAH molecules for experimental guidance. According to the linear equation in red (Figure 9), the HMO localization energy of 3.6 corresponds to a reaction free energy of about 0 kcal/mol. We set the localization energy of 3.6 as the critical value. Only reaction sites with localization energies lower than 3.6 are able to undergo DA reactions with fullerene.

We further explored other aromatic molecules composed of one or two rows of pentacene or tetracene with all the possible arrangements. Their chemical structures and HMO localization energies of different diene sites are listed in Figure 8. The reaction sites with localization energies lower than 3.6 are highlighted in red.

To test the applicability of two linear equations shown in Figure 9, we applied them to five reactive sites (E_L < 3.6) of another three PAHs (b, h, and i shown in Figure 8). Based on their HMO localization energies, the derived activation free energies (ΔG_{act}-D) and reaction free energies (ΔG_{rxn}-D) in cycloadditions with [60]fullerene were obtained (Table 1). For

Table 1. Comparison of Activation Free Energies and Reaction Free Energies Derived (ΔG_{act}-D and ΔG_{rxn}-D, in kcal/mol) from Linear Equations (Figure 9) and Those (ΔG_{act} and ΔG_{rxn}, in kcal/mol) from DFT Calculations

PAH_site	E_L ($-\beta$)	ΔG_{act}-D	ΔG_{act}	ΔG_{rxn}-D	ΔG_{rxn}
b_2	3.27	21.0	22.0	−12.1	−9.7
b_3	3.32	21.7	22.2	−10.3	−9.2
h_2	3.26	20.9	20.9	−12.4	−12.2
h_3	3.28	21.2	18.7	−11.7	−15.5
i_2	3.34	22.0	21.3	−9.6	−10.5

comparison, the corresponding values from DFT calculations are listed as ΔG_{act} and ΔG_{rxn} in Table 1. For activation free energies, the differences between the HMO method and the M06-2X method are in the range of 2.5 to −1.0 kcal/mol. Similarly, the differences of reaction free energies are in the range of 3.8 to −2.4 kcal/mol. These results demonstrate that the simple HMO method can be of considerable value in estimating reaction barriers and thermodynamics.

CONCLUSION

The Diels−Alder reactions of C_{60} with pentacene, bistetracene, and their bis(2-trimethylsilylethynyl)-substituted derivatives have been studied by density functional theory calculations. For pentacene, the reaction on the central diene site 3 is favorable both kinetically and thermodynamically. For TMS-PT, the substituent groups on site 3 have a strong influence only on the stability of product **TMS-PT_P3**. The formation of **TMS-PT_P3** is still kinetically favored, which is validated by NMR experiments at room temperature. Under thermodynamically controlled conditions (refluxing in CS_2 for 24 h), the most stable adduct on site 2 (**TMS-PT_P2**) is obtained as the major product. For BT, the two-row fused aromatic ring framework deactivates the molecule toward DA reactions. The DA barriers are significantly higher than those with pentacene. Site 2 in BT is the most reactive one among four reaction sites, and only the reaction on site 2 is exergonic. The additional side groups slightly affect the reaction barriers with TMS-BT, which are quite close to those with BT. One silylethynyl substituent on site 3 can further destabilize the stability of the corresponding adduct (**TMS-BT_P3**) by about 6 kcal/mol. In addition, calculations show that TMS-BT is about 5 orders of magnitude less reactive than TMS-PT in the reactions with fullerene. This accounts for the chemical inertness of the TIPS-BT molecule. We also investigated the localization energies of different sites in a series of PAHs based on the HMO method. We found that the HMO localization energies can be used to estimate the reactivities of various PAH molecules in cycloadditions with fullerenes. Our study provides valuable insight into the design of stable, unconventional linear PAHs for organic electronic applications.

dx.doi.org/10.1021/ja505240e | J. Am. Chem. Soc. 2014, 136, 10743−10751

■ ASSOCIATED CONTENT

Supporting Information

Figure S1, Table S1, and details of computations and experiments. This material is available free of charge via the Internet at http://pubs.acs.org.

■ AUTHOR INFORMATION

Corresponding Authors

abriseno@mail.pse.umass.edu
houk@chem.ucla.edu

Notes

The authors declare no competing financial interest.

■ ACKNOWLEDGMENTS

We are grateful to the National Science Foundation (CHE-1059084 to K.N.H.) for financial support of this research. L.Z. and A.L.B acknowledge support from the Office of Naval Research (N000141110636). S.O. acknowledges the European Community for postdoctoral fellowships (PIOF-GA-2009-252856 and PCIG14-GA-2013-630978) and the Spanish MINECO for JdC contract JCI-2012-14438. Calculations were performed on the Hoffman2 cluster at UCLA and the Extreme Science and Engineering Discovery Environment (XSEDE), which is supported by the NSF (OCI-1053575).

■ REFERENCES

(1) Anthony, J. E. *Angew. Chem., Int. Ed.* **2008**, *47*, 452.
(2) Yoo, S.; Domercq, B.; Kippelen, B. *Appl. Phys. Lett.* **2004**, *85*, 5427.
(3) Jurchescu, O. D.; Baas, J.; Palstra, T. T. M. *Appl. Phys. Lett.* **2004**, *84*, 3061.
(4) Yi, Y.; Coropceanu, V.; Brédas, J.-L. *J. Am. Chem. Soc.* **2009**, *131*, 15777.
(5) Congreve, D. N.; Lee, J.; Thompson, N. J.; Hontz, E.; Yost, S. R.; Reusswig, P. D.; Bahlke, M. E.; Reineke, S.; Van Voorhis, T.; Baldo, M. A. *Science* **2013**, *340*, 334.
(6) Yamada, M.; Ikemote, I.; Kuroda, H. *Bull. Chem. Soc. Jpn.* **1988**, *61*, 1057.
(7) Takahashi, T.; Kitamura, M.; Shen, B. J.; Nakajima, K. *J. Am. Chem. Soc.* **2000**, *122*, 12876.
(8) Mack, J.; Miller, G. P. *Fullerene Sci., Technol.* **1997**, *5*, 607.
(9) (a) Miller, G. P.; Mack, J. *Org. Lett.* **2000**, *2*, 3979. (b) Miller, G. P.; Mack, J.; Briggs, J. B. *Org. Lett.* **2000**, *2*, 3983. (c) Miller, G. P.; Briggs, J. B. *C.R. Chim.* **2006**, *9*, 916. (d) Kaur, I.; Miller, G. P. *New J. Chem.* **2008**, *32*, 459.
(10) (a) Kaur, I.; Jia, W.; Kopreski, R.; Selvarasah, S.; Dokmeci, M. R.; Pramanik, C.; McGruer, N.; Miller, G. P. *J. Am. Chem. Soc.* **2008**, *130*, 16274. (b) Fudickar, W.; Linker, T. *J. Am. Chem. Soc.* **2012**, *134*, 15071.
(11) (a) Payne, M. M.; Parkin, S. R.; Anthony, J. E. *J. Am. Chem. Soc.* **2005**, *127*, 8028. (b) Chun, D.; Cheng, Y.; Wudl, F. *Angew. Chem., Int. Ed.* **2008**, *47*, 8380. (c) Xiao, J. C.; Duong, H. M.; Liu, Y.; Shi, W. X.; Li, G.; Li, S. Z.; Liu, X. W.; Ma, J.; Wudl, F.; Zhang, Q. C. *Angew. Chem., Int. Ed.* **2012**, *51*, 6094.
(12) (a) Zhang, L.; Fonari, A.; Zhang, Y.; Zhao, G.; Coropceanu, V.; Hu, W.; Parkin, S.; Brédas, J.−L.; Briseno, A. L. *Chem.—Eur. J.* **2013**, *19*, 17907. (b) Zhang, L.; Walker, B.; Liu, F.; Colella, N. S.; Mannsfeld, S. C. B.; Watkins, J. J.; Nguyen, T.-Q.; Briseno, A. L. *J. Mater. Chem.* **2012**, *22*, 4266.
(13) Zhang, L.; Fonari, A.; Liu, Y.; Hoyt, A.-L. M.; Lee, H.; Granger, D.; Parkin, S.; Russell, T. P.; Anthony, J. E.; Brédas, J.-L.; Coropceanu, V.; Briseno, A. L. *J. Am. Chem. Soc.* **2014**, *136*, 9248.
(14) Biermann, D.; Schmidt, W. *J. Am. Chem. Soc.* **1980**, *102*, 3173.
(15) Frisch, M. J.; Trucks, G. W.; Schlegel, H. B.; Scuseria, G. E.; Robb, M. A.; Cheeseman, J. R.; Scalmani, G.; Barone, V.; Mennucci, B.; Petersson, G. A.; Nakatsuji, H.; Caricato, M.; Li, X.; Hratchian, H. P.; Izmaylov, A. F.; Bloino, J.; Zheng, G.; Sonnenberg, J. L.; Hada, M.; Ehara, M.; Toyota, K.; Fukuda, R.; Hasegawa, J.; Ishida, M.; Nakajima, T.; Honda, Y.; Kitao, O.; Nakai, H.; Vreven, T.; Montgomery, J. A., Jr.; Peralta, J. E.; Ogliaro, F.; Bearpark, M.; Heyd, J. J.; Brothers, E.; Kudin, K. N.; Staroverov, V. N.; Keith, T.; Kobayashi, R.; Normand, J.; Raghavachari, K.; Rendell, A.; Burant, J. C.; Iyengar, S. S.; Tomasi, J.; Cossi, M.; Rega, N.; Millam, J. M.; Klene, M.; Knox, J. E.; Cross, J. B.; Bakken, V.; Adamo, C.; Jaramillo, J.; Gomperts, R.; Stratmann, R. E.; Yazyev, O.; Austin, A. J.; Cammi, R.; Pomelli, C.; Ochterski, J. W.; Martin, R. L.; Morokuma, K.; Zakrzewski, V. G.; Voth, G. A.; Salvador, P.; Dannenberg, J. J.; Dapprich, S.; Daniels, A. D.; Farkas, O.; Foresman, J. B.; Ortiz, J. V.; Cioslowski, J.; Fox, D. J. *Gaussian 09*, revision D.01; Gaussian Inc.: Wallingford, CT, 2013.
(16) Yang, T.; Zhao, X.; Nagase, S. *Org. Lett.* **2013**, *15*, 5960.
(17) (a) Becke, A. D. *Phys. Rev. A* **1988**, *38*, 3098. (b) Becke, A. D. *J. Chem. Phys.* **1993**, *98*, 5648. (c) Lee, C.; Yang, W.; Parr, R. G. *Phys. Rev. B* **1988**, *37*, 785.
(18) (a) Hariharan, P. C.; Pople, J. A. *Theor. Chim. Acta* **1973**, *28*, 213. (b) Hehre, W. J.; Ditchfield, R.; Pople, J. A. *J. Chem. Phys.* **1972**, *56*, 2257.
(19) (a) Osuna, S.; Swart, M.; Solà, M. *J. Phys. Chem. A* **2011**, *115*, 3491. (b) Garcia-Borràs, M.; Osuna, S.; Swart, M.; Luis, J. M.; Solà, M. *Chem. Commun.* **2013**, *49*, 1220.
(20) (a) Chai, J.-D.; Head-Gordon, M. *Phys. Chem. Chem. Phys.* **2008**, *10*, 6615. (b) Fokin, A. A.; Chernish, L. V.; Gunchenko, P. A.; Tikhonchuk, E. Y.; Hausmann, H.; Serafin, M.; Dahl, J. E.; Carlson, R. M.; Schreiner, P. R. *J. Am. Chem. Soc.* **2012**, *134*, 13641.
(21) (a) Zhao, Y.; Truhlar, D. G. *Theor. Chem. Acc.* **2008**, *120*, 215. (b) Zhao, Y.; Truhlar, D. G. *Acc. Chem. Res.* **2008**, *41*, 157.
(22) (a) Paton, R. S.; Mackey, J. L.; Kim, W. H.; Lee, J. H.; Danishefsky, S. J.; Houk, K. N. *J. Am. Chem. Soc.* **2010**, *132*, 9335. (b) Lan, Y.; Zou, L.-F.; Cao, Y.; Houk, K. N. *J. Phys. Chem. A* **2011**, *115*, 13906.
(23) (a) Bian, S.; Scott, A. M.; Cao, Y.; Liang, Y.; Osuna, S.; Houk, K. N.; Braunschweig, A. B. *J. Am. Chem. Soc.* **2013**, *135*, 9240. (b) Cao, Y.; Osuna, S.; Liang, Y.; Haddon, R. C.; Houk, K. N. *J. Am. Chem. Soc.* **2013**, *135*, 17643. (c) Lazar, P.; Karlický, F.; Jurečka, P.; Kocman, M.; Otyepková, E.; Šafářová, K.; Otyepka, M. *J. Am. Chem. Soc.* **2013**, *135*, 6372.
(24) (a) Barone, V.; Cossi, M. *J. Phys. Chem. A* **1998**, *102*, 1995. (b) Cossi, M.; Rega, N.; Scalmani, G.; Barone, V. *J. Comput. Chem.* **2003**, *24*, 669. (c) Takano, Y.; Houk, K. N. *J. Chem. Theory Comput.* **2005**, *1*, 70.
(25) Grimme, S. *WIREs Comput. Mol. Sci.* **2011**, *1*, 211.
(26) (a) Ess, D. H.; Houk, K. N. *J. Am. Chem. Soc.* **2007**, *129*, 10646. (b) Legault, C. Y.; Garcia, Y.; Merlic, G. A.; Houk, K. N. *J. Am. Chem. Soc.* **2007**, *129*, 12664. (c) Ess, D. H.; Houk, K. N. *J. Am. Chem. Soc.* **2008**, *130*, 10187.
(27) For reviews, see: (a) van Zeist, W.-J.; Bickelhaupt, F. M. *Org. Biomol. Chem.* **2010**, *8*, 3118. (b) Fernández, I. *Phys. Chem. Chem. Phys.* **2014**, *16*, 7662.
(28) (a) Fernández, I.; Bickelhaupt, F. M. *J. Comput. Chem.* **2012**, *33*, 509. (b) Gordon, C. G.; Mackey, J. L.; Jewett, J. C.; Sletten, E. M.; Houk, K. N.; Bertozzi, C. R. *J. Am. Chem. Soc.* **2012**, *134*, 9199. (c) Liang, Y.; Mackey, J. L.; Lopez, S. A.; Liu, F.; Houk, K. N. *J. Am. Chem. Soc.* **2012**, *134*, 17904. (d) Fernández, I.; Bickelhaupt, F. M.; Cossío, F. P. *Chem.—Eur. J.* **2012**, *18*, 12395. (e) Lopez, S. A.; Houk, K. N. *J. Org. Chem.* **2013**, *78*, 1778. (f) Zou, L.; Paton, R. S.; Eschenmoser, A.; Newhouse, T. R.; Baran, P. S.; Houk, K. N. *J. Org. Chem.* **2013**, *78*, 4037. (g) Fernández, I.; Solà, M.; Bickelhaupt, F. M. *Chem.—Eur. J.* **2013**, *19*, 7416. (h) Kamber, D. N.; Nazarova, L. A.; Liang, Y.; Lopez, S. A.; Patterson, D. M.; Shih, H.-W.; Houk, K. N.; Prescher, J. A. *J. Am. Chem. Soc.* **2013**, *135*, 13680. (i) Liu, F.; Paton, R. S.; Kim, S.; Liang, Y.; Houk, K. N. *J. Am. Chem. Soc.* **2013**, *135*, 15642. (j) Usharani, D.; Lacy, D. C.; Borovik, A. S.; Shaik, S. *J. Am. Chem. Soc.* **2013**, *135*, 17090. (k) Hong, X.; Liang, Y.; Griffith, A. K.; Lambert, T. H.; Houk, K. N. *Chem. Sci.* **2014**, *5*, 471. (l) Yang, Y.-F.; Cheng, G.-J.; Liu, P.; Leow, D.; Sun, T.-Y.; Chen, P.; Zhang, X.; Yu, J.-Q.; Wu, Y.-D.; Houk, K. N. *J. Am. Chem. Soc.* **2014**, *136*, 344. (m) Hong, X.; Liang,

Y.; Houk, K. N. *J. Am. Chem. Soc.* **2014**, *136*, 2017. (n) Fernández, I.; Bickelhaupt, F. M. *J. Comput. Chem.* **2014**, *35*, 371. (o) Yang, J.; Liang, Y.; Šečkutė, J.; Houk, K. N.; Devaraj, N. K. *Chem.—Eur. J.* **2014**, *20*, 3365. (p) Liu, S.; Lei, Y.; Qi, X.; Lan, Y. *J. Phys. Chem. A* **2014**, *118*, 2638.

(29) Hirsch, A.; Brettreich, M. *Fullerenes: Chemistry and Reactions*; Wiley-VCH: Weinheim, 2004.

(30) Slanina, Z.; Stobinski, L.; Tomasik, P.; Lin, H.-M.; Adamowicz, L. *J. Nanosci. Nanotechnol.* **2003**, *3*, 193.

(31) Wheland, G. W. *J. Am. Chem. Soc.* **1942**, *64*, 900.

(32) Brown, R. D. *Q. Rev. Chem. Soc.* **1952**, *6*, 63.

(33) For the relationship between distortion energies and the DA reactivities of PAHs, see: Hayden, A. E.; Houk, K. N. *J. Am. Chem. Soc.* **2009**, *131*, 4084.

(34) Schleyer, P. v. R.; Manoharan, M.; Jiao, H.; Stahl, F. *Org. Lett.* **2001**, *3*, 3643.

(35) http://www.chem.ucalgary.ca/SHMO/.